conditions are independent of Reynolds number and $u_\infty^2/I_\infty$ is fixed. Also, $\theta/L\ Re_L^{n/n+1}$, $\delta^*/L\ Re_L^{n/n+1}$ and the other nondimensional thicknesses are independent of $Re_L$. Moreover, the local shear stress and local heat transfer vary as $Re_L^{-n/n+1}$; therefore the total friction stress and the total heat transfer vary as $Re_L^{-n/n+1}$ if the boundary layer is either entirely laminar or entirely turbulent.

Because $\tau_*$ is independent of Reynolds number, the skin-friction drops to zero at a value of $x/L$ that is independent of Reynolds number. Therefore, the separation point also is independent of Reynolds number. The same conclusion follows from the result that the nondimensional velocity profiles are independent of Reynolds number. For these results to be correct, the friction coefficient must be expressible as a power function of $Re_\theta$; this is exact for laminar flow but only approximate for turbulent flow. Moreover, the nondimensional velocity profiles and the nondimensional thicknesses at the initial point of the boundary layer must be independent of Reynolds number.

If $Q_{*w} = 0$, $u_\infty^2/I_\infty$ fixed, and the other boundary conditions made independent of $Re_L$ a solution of the nondimensional equations gives $I_{*a}(x_*)$, the value for zero heat transfer. Under these conditions, $I_{*a}(x_*)$ is independent of $Re_L$. From the definition of the recovery factor $r$, it follows that

$$I_{*a}(x_*) = I_{*e}(x_*) - (u_{*e}^2/2)(1 - r)(u_\infty^2/I_\infty)$$

Therefore when $u_\infty^2/I_\infty$ is fixed and the boundary conditions are independent of $Re_L$ the recovery factor is independent of $Re_L$.

By using Eqs. (5), (6), and (9) with $\rho_e = \rho_{e1}$, $u_e = u_{e1}$, there is obtained

$$C_{f1}Re_{x1}^{n/(n+1)} = C_fRe_x^{n/(n+1)}\left[\int_0^{x/L}\left(\frac{r_w}{L}\right)^{n+1} d\frac{x}{L}\Big/\frac{x}{L}\left(\frac{r_w}{L}\right)^{n+1}\right]^{n/(n+1)} \quad (13)$$

at corresponding $x$ and $x_1$. A relation for Stanton numbers is obtained from Eq. (13) by replacing $C_f$ by $St$ and $C_{f1}$ by $St_1$. Relations between various boundary-layer thicknesses in axisymmetric and two-dimensional flows are derived in the same way.

For a cone, $r_w/L = ax/L$ and $\rho_e$ and $u_e$ are constant. Because $\rho_e = \rho_{e1}$ and $u_e = u_{e1}$, $\rho_{e1}$ and $u_{e1}$ also are constant. Therefore the corresponding two-dimensional flow is that over a flat plate at zero angle of attack. Equation (13) then becomes

$$C_{f1}Re_{x1}^{n/(n+1)} = C_fRe_x^{n/(n+1)}(n + 2)^{-n/(n+1)} \quad (14)$$

at corresponding $x$ and $x_1$ with $M_e = M_{e1}$, $T_e = T_{e1}$, $T_w = T_{w1}$, $p_e = p_{e1}$.

For a plate or cone with constant surface temperature the reference length $L$ can be replaced by $x$. Therefore, the conclusion that the local shear stress varies as $Re_L^{-n/n+1}$ can be expressed as

$$C_{f1}Re_{x1}^{n/(n+1)} = C_1 \text{ and } C_fRe_x^{n/(n+1)} = C_2$$

Consequently, $C_{f1}Re_{x1}^{n/(n+1)}$ is independent of $x_1$ and $C_fRe_x^{n/(n+1)}$ is independent of $x$. Therefore Eq. (14) holds for all combinations of $x$ and $x_1$. In particular for $Re_f = Re_{x1}$

$$C_f/C_{f1} = (n + 2)^{n/(n+1)} \quad (15)$$

and for

$$C_f = C_{f1},$$
$$Re_{x1}/Re_x = 1/(n + 2) \quad (16)$$

These relations are usually obtained by using the boundary-layer momentum equation for a cone and that for a plate, together with a power law friction formula, and the assumption of similar velocity profiles on cone and plate.

Van Driest[6] obtains the relation

$$Re_{x1}/Re_x = \tfrac{1}{2} \quad (17)$$

for turbulent flow instead of Eq. (16). In going from Eq. (16) to Eq. (17) of Ref. 6 and from Eq. (19) to Eq. (20) of Ref. 6, it was assumed that a quantity "$a$" was very large. This means that $C_f$ was very small and thus that $Re_\theta$ was very large. Because the rate of decrease of $C_f$ with increase in Reynolds number decreases as the Reynolds number increases, $n \to 0$ as $Re_\theta \to \infty$. Then Eq. (16) approaches Eq. (17). Therefore Eq. (17) is a limiting relation for very large $Re_\theta$.

By taking the boundary conditions at infinity for the cone boundary layer to be those at the outer edge of the boundary layer and equal to those at the outer edge of the flat plate boundary layer, it can be shown that the recovery factor on a cone equals that on a flat plate and that both are independent of Reynolds number.

### References


[1] Mangler, W., "Zusammenhang Zwischen ebenen und rotationssymmetrischen Grenzschichten in kompressiblen Flussigkeiten," *Zeitschrift fuer Angewandte Mathematik und Physik*, Vol. 28, 1948, pp. 97–103.

[2] Mangler, W., Rept. 45-A-17, Aerodynamische Versuchanstalt; also Göttingen, E. V., British Reports and Translations No. 55, April 1946, M.A.P., Vokenrode.

[3] Tetervin, N., "A Generalization to Turbulent Boundary Layers of Mangler's Transformation Between Axisymmetric and Two-Dimensional Laminar Boundary Layers," NOLTR 69–47, 1969, U.S. Naval Ordnance Lab., White Oak, Md.

[4] Schlichting, H., *Boundary Layer Theory*, 6th ed., McGraw-Hill, New York, 1968.

[5] Sasman, P. K. and Cresci, R. J., "Compressible Turbulent Boundary Layer with Pressure Gradient and Heat Transfer," *AIAA Journal*, Vol. 4, No. 1, Jan. 1966, pp. 19–25.

[6] Van Driest, E. R., "Turbulent Boundary Layer on a Cone in a Supersonic Flow at Zero Angle of Attack," *Journal of Aeronautical Sciences*, Vol. 19, No. 1, 1952.


## Some Effects of Acceleration on the Turbulent Boundary Layer


PAUL F. BRINICH* AND HARVEY E. NEUMANN†
*NASA Lewis Research Center, Cleveland, Ohio*


IMPLICIT in most boundary-layer analyses is the assumption that the boundary layer entrains fluid from the free-stream, i.e., that the proper outer edge condition for the boundary layer is the local freestream. That this is not necessarily true has been demonstrated in the case of supersonic flow over blunted bodies where the boundary-layer development takes place within the shock layer formed by a leading edge bow shock.[1] An attempt will be made in the present Note to demonstrate experimentally that boundary-layer entrainment of the local freestream also may not be a valid assumption for the case of strongly accelerated flows in general. In this instance, the boundary-layer thinning can become so severe that the boundary layer may be considered to develop within the wake of the upstream boundary layer rather than in the freestream.

### Experimental Procedure

Boundary-layer profiles and wall-static pressures were measured in the two-dimensional convergent-divergent test

Received October 23, 1969; revision received January 28, 1970.

* Aerospace Research Engineers, Fundamental Heat Transfer Branch.

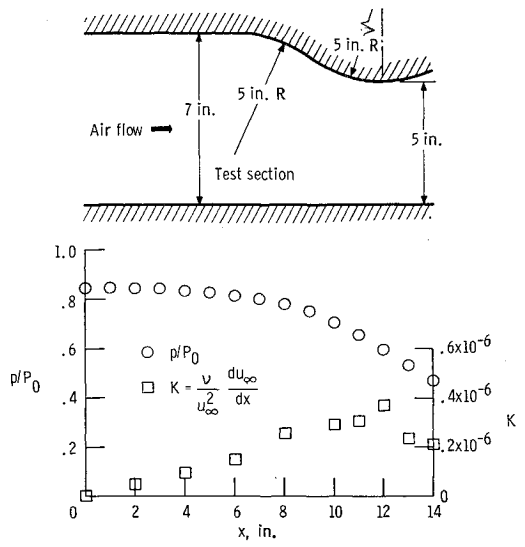


**Fig. 1 Test section configuration and pressure distribution on flat wall.**

section shown in Fig. 1. This section was preceded by a constant area channel about 36 in. long having a smooth bell mouth entrance. The channel height normal to the page was about 4 in., and other pertinent dimensions are indicated in Fig. 1. Velocity profiles were measured with conventional boundary-layer Pitot tubes on both the flat and curved walls at about 1-in. intervals for a distance of 14 in. along the channel. In this Note, only those profiles measured along the flat wall will be analyzed since they were free of secondary flows and had negligible static-pressure gradients normal to the wall. It should be pointed out, however, that the curved-wall measurements, which were obtained in a region of much stronger acceleration, showed the same trends as those on the flat wall. Test conditions were such that choked flow was maintained in the throat region and near atmospheric pressure and 80°F temperatures in the plenum.

## Results

The static-pressure distribution along the flat wall in the boundary-layer survey region is shown at the bottom of Fig. 1, where the static pressure is nondimensionalized by the plenum pressure. This distribution indicates a positively accelerating flow throughout the test region. The pressure gradient parameter $K$ (Ref. 2) given by

$$K = \nu_w/u_\infty^2 \, du_\infty/dx$$

also is shown in Fig. 1. Its maximum value of $0.38 \times 10^{-6}$ at $x = 12$ suggests that the flow is still turbulent, since a value almost ten times larger is considered necessary to laminarize the flow.

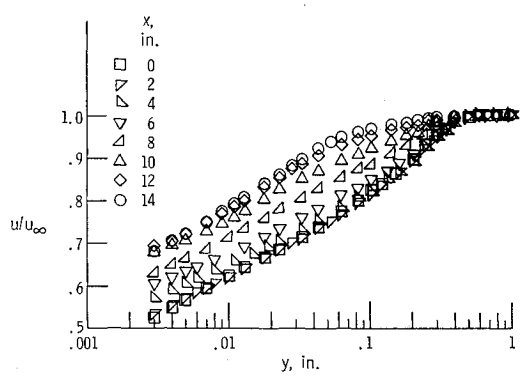


**Fig. 2 Velocity profiles along flat wall.**

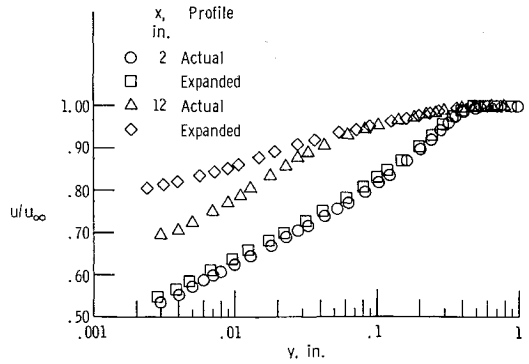


**Fig. 3 Comparison of actual and expanded velocity profiles.**

The velocity profiles for the flat wall at 2-in. intervals are shown in Fig. 2 as the local velocity divided by the freestream velocity $u/u_\infty$, against the distance normal to the wall, $y$, in inches. A semilog plot was used to determine how well the straight line relation predicted by the law of the wall was matched by the measured profiles and how the flow acceleration modified this relation. Figure 2 shows that the essentially linear portion of the initial velocity profiles at $x = 0$ and 2 in. extends out as far as $y = 0.07$ in. Beyond this point, the formation of the intermittent wake region and its attendent higher velocities is apparent. In proceeding farther downstream, the linear portion of the profile increases in extent toward the freestream until at $x = 8$ in. the entire profile becomes more or less linear, indicating a disappearance of the outer-wake region. The $x = 8$ profile appears similar to a fully developed turbulent pipe profile, with the exception that in the present instance the profile was generated in an accelerating flow rather than in a constant velocity pipe. Beginning with the $x = 8$ in. profile and continuing downstream, it is apparent that the outer-wake region has been replaced with a region having appreciably smaller velocity gradients.

If the initial profiles of Fig. 2 were expressed in terms of power laws, an exponent of $\frac{1}{8}$ would be a good representation over most of the profile. At the downstream locations, the inner 20% also can be represented by a $\frac{1}{8}$ power whereas the outer 80% has changed to a $\frac{1}{10}$ power fit. A close examination of the $x \geq 8$ in. profiles shows that around $y \sim 0.03$ in. there is a region of upward concavity, or increasing velocity gradient, which suggests a new wake-like region much closer to the wall. It is interesting to note that in an independent experiment at Lewis involving accelerated flow in a nozzle,[3] intermittency measurements revealed an intermittent wake-like structure near the wall imbedded in a much larger intermittent wake-like outer region, suggesting the presence of two rather distinct layers. The power law behavior of the profile in Ref. 3 was similar to that reported for the present Note. Such observations lead one to question to what extent the entire velocity profile is influenced by frictional as well as pressure forces.

It is well known that when a boundary layer is subjected to a strong positive acceleration the shear stress normal to the wall drops off very rapidly, leaving much of the outer profile with a very small shear gradient $\partial\tau/\partial y$. This means that at some point in the velocity profile the shear-stress gradient may become negligible compared to the favorable pressure gradient and the flow will be representable as an inviscid rotational flowfield out to the freestream. That this does indeed happen can be shown by comparing an actual velocity profile with a hypothetical profile which has been obtained by neglecting the frictional contribution. Such a profile can be formed by considering a boundary-layer total-pressure profile measured at some upstream station together with the static pressure at the (downstream) station in question and

computing a velocity profile. This profile, referred to as an expanded profile, then can be compared to the actual profile observed at the downstream station. The velocity differences between the two profiles are indicative of the local shear gradient $\partial\tau/\partial y$ in the boundary layer.

Such comparisons of actual and expanded profiles are shown in Fig. 3. The actual profile at $x = 2$ and at $x = 12$ were taken from Fig. 2. The expanded profiles, on the other hand, were computed using the total pressure surveys at $x = 0$ and $x = 10$ and the static pressures at $x = 2$ and $x = 12$ respectively, and have an adjustment on $y$ incorporated into them to satisfy the condition that the total pressure remains constant along streamlines (rather than along lines of constant $y$). The expanded profiles are hypothetical velocity profiles that would exist at $x = 2$ and $x = 12$ if there were no dissipative processes from $x = 0$ to $x = 2$ and from $x = 10$ to $x = 12$ in. Thus, any velocity differences between the actual profiles and the expanded profiles in Fig. 3 will be caused by shear effects.

In comparing the $x = 2$ actual and expanded profiles, it is apparent that a small but measurable velocity difference exists over the greater part of the velocity profile, indicating the presence of turbulent dissipation throughout the entire boundary layer. Such behavior is typical of boundary-layer profiles in zero or slightly favorable pressure gradients. A comparison of the $x = 12$ actual and expanded profiles, however, shows some remarkable contrasts. The small velocity differences characteristic of the $x = 2$ profiles now have vanished over the outer part of the profile, but have increased greatly in the region of the wall. The dissipative processes now are concentrated in the inner 20% of the profile, leaving the outer 80% virtually friction free. The shape of the outer part of the profile now results from an inviscid expansion of an upstream total pressure profile obtained where the pressure gradient was smaller.

The two examples shown in Fig. 3 were chosen because they represented typical boundary-layer behaviors for small and large favorable pressure gradients. Similar comparisons of actual and expanded velocity profiles have been made for all the velocity profiles shown in Fig. 2 and will be reported in a more complete study. These comparisons indicated that for profiles up to about $x = 8$ in., velocity differences between the actual and the expanded profiles existed over the entire boundary-layer thickness with somewhat more marked differences near the wall. For $x > 8$ in., the velocity differences in the outer 80% of the profile disappeared and were replaced with much increased differences at the wall.

In view of the large reduction in the thickness of the frictional part of the velocity profile as the flow accelerated (from $\delta \sim 0.5$ at $x = 0$ to $\delta \sim 0.1$ in. at $x = 12$ in.), it is of interest to consider what changes in mass flow have occurred. A comparison of the $x = 12$ in. with the $x = 0$ profile reveals about a 70% reduction in the frictional layer mass flow. A similar comparison using the integral method of Ref. 4 indicates a 60% reduction in boundary-layer mass flow for the present configuration (Ref. 4 incidentally was found to predict the momentum and displacement thicknesses within 10%). The observed velocity profiles and the associated reduction in mass-flow content of the frictional boundary layer therefore suggests the formation of a self-generated wake-like region having negligible shear gradients and extending from the outer edge of the frictional boundary layer to the freestream.

The analysis of the profiles on the curved wall shows the same general characteristics noted previously for the flat wall. However, because of the stronger pressure gradients, the inviscid part of the velocity profiles extended over approximately 95% of the layer, leaving only 5% of the layer where turbulent dissipation could be measured (as indicated by losses in total pressure). The maximum value of the pressure gradient parameter $K$ was $1.2 \times 10^{-6}$ for the curved wall, which is still one third of the value suggested for laminarization. Extrapolation of the curved wall results to still larger pressure gradients may indicate an extension of the inviscid outer layer into the region of the laminar sublayer, which then may account for the laminarization of the turbulent boundary layer under the proper conditions.

The development of the turbulent boundary layer in a favorable pressure gradient as described in this Note may have important implications especially in regard to the transfer of heat. If the outer-wake region is attenuated or disappears, then an important mechanism for the transport of heat from the freestream has been modified, and the turbulent heat-transfer rate should be altered from its normal value. If the acceleration is great enough to cause laminarization of the boundary layer, then heat-transfer characteristic of laminar flow should be observed. That such heat-transfer variations actually do exist has been demonstrated by Boldman[5] and others in their investigation of heat transfer in a converging-diverging nozzle.

### References

[1] Brinich, P. F., "Effect of Leading Edge Geometry on Boundary-Layer Transition at M = 3.1," TN 3659, 1956, NACA.

[2] Schraub, F. A. and Kline, S. J., "A Study of the Structure of the Turbulent Boundary Layer with and without Longitudinal Pressure Gradients," Rept. MD-12, 1965, Stanford Univ., Stanford, Calif.

[3] Boldman, D. R., Neumann, H. E., and Ehlers, R. C., "Velocity, Intermittency, and Turbulence Intensity Measurements in the Boundary Layer of an Accelerated Flow," TM to be published.

[4] Elliott, D. G., Bartz, D. R., and Silver, D., "Calculation of Turbulent Boundary-Layer Growth and Heat Transfer in Axisymmetric Nozzles," TR. 32-387, 1963, Jet Propulsion Lab., California Institute of Technology, Pasadena, Calif.

[5] Boldman, D. R., Schmidt, J. F., and Gallagher, A. K., "Laminarization of a Turbulent Boundary Layer as Observed from Heat-Transfer and Boundary-Layer Measurements in Conical Nozzles," TN D-4788, 1968, NASA.